Dynamic Countermeasure Fabrics for Post-Spaceflight Orthostatic Intolerance

Rachael M. Granberry; Kevin P. Eschen; Amy J. Ross; Julianna M. Abel; Bradley T. Holschuh

INTRODUCTION: Aerospace orthostatic intolerance garments (OIG) have historically been pneumatic (e.g., NASA's antigravity suit), an approach that inhibits mobility and requires connection to an air supply. Elastic compression garments, an alternative technology, are difficult to don/doff and cannot be worn in a noncompressive state, resulting in discomfort and usability challenges. This research evaluates a novel technology—contractile shape memory alloy (SMA) knitted actuators—that can enable low-profile, dynamic compression for an aerospace OIG.

METHODS: To characterize the functional capabilities of SMA knitted actuators, displacement control testing was conducted on 10 actuator samples with a range of geometric design parameters. Inactive (F_I) and actuated forces (F_A) were observed by repeatedly thermally cycling each sample at 0%, 15%, 30%, and 45% structural strain. Compression capabilities were approximated using medical compression hosiery standards and anthropometric data from a representative aerospace population (ANSUR 2012).

RESULTS: Dynamic compression predictions reached 52 mmHg (single layer fabric) and 105 mmHg (double layer fabric) at the ankle. Low, inactive pressures ($p < 20$ mmHg) demonstrate that compression is controllable and can be dynamically increased upon actuation up to 33 mmHg in a single layer system and up to 67 mmHg in a double layer system.

DISCUSSION: The results highlight the potential of SMA knitted actuators to enable low-profile, dynamic compression garments that can reach medically therapeutic pressures on an aerospace population to counteract OI symptoms. In addition to astronautic applications, this technology demonstrates widespread terrestrial medical and high-performance aircraft applicability.

KEYWORDS: orthostatic intolerance, medical compression, shape memory alloys, functional fabrics.

Granberry RM, Eschen KP, Ross AJ, Abel JM, Holschuh BT. *Dynamic countermeasure fabrics for post-spaceflight orthostatic intolerance*. Aerosp Med Hum Perform. 2020; 91(6):525–531.

Lower-body compression garments are widely used in aerospace medicine to support the cardiovascular system by preventing blood pooling in the lower body and facilitating venous return. Without positive counterpressure, astronauts risk presyncopal symptoms from post-spaceflight orthostatic intolerance (OI), a condition experienced by 20–60% of astronauts returning from short-duration space missions and up to 83% of those returning from missions lasting over 1 mo.[7] OI symptoms can persist several days after landing and are caused by cardiac deconditioning, loss of plasma volume, fluid shifting, and loss of baroreceptor sensitivity.[6] OI symptoms are statistically higher in women (5:1) and the difference between sexes could be attributed to a number of biological factors, including lower centers of mass, lower vascular resistance, lower plasma volume, and lower mean arterial pressure due to a vasodilatory response to estrogen.[12] While countermeasures, such as exercise, fluid loading, and countermaneuvers, can mitigate OI symptoms, these measures do not eliminate risk and, consequently, astronauts and cosmonauts are required to wear lower body compression garments during Earth reentry, landing, and egress.[10]

NASA's Commercial Crew Program requires mean lower body positive pressure between 40–80 mmHg (5.3–10.7 kPa) for orthostatic protection post-spaceflight.[8] NASA's antigravity

From the University of Minnesota, Minneapolis, MN, USA, and NASA Johnson Space Center, Houston, TX, USA.

This manuscript was received for review in November 2019. It was accepted for publication in March 2020.

Address correspondence to: Rachael M. Granberry, 240 McNeal Hall, 1985 Buford Ave., Saint Paul, MN 55108; granb017@umn.edu.

DOI: https://doi.org/10.3357/AMHP.5560.2020

suit is a pneumatic compression garment used during the shuttle program that provides on-body compression up to 78 mmHg (1.5 psi) in 26 mmHg (0.5 psi) increments.[7] The Russian kentavr is an alternative OI garment that uses tensioned elastic fabric to produce an average pressure of 30 mmHg around the lower body, which can be adjusted through lateral laces.[6] NASA researchers designed a gradient compression garment (GCG) to reduce or eliminate the risks associated with the antigravity suit, such as mobility impairment and chance of deflation.[7] The GCG is an elastic, custom-fit garment that provides 55 mmHg (7.3 kPa) at the ankle, 35 mmHg (4.7 kPa) at the knee, 18 mmHg (2.4 kPa) at the thigh, and 16 mmHg (2.1 kPa) at the abdomen.[11] The GCG has been validated through clinical trials as effective in preventing OI symptoms;[11] however, the semistatic design, which includes modular zipper panels at the waist, limits the user's ability to wear the garment unpressurized before landing activities are initiated or modify pressure in response to changing environmental or physiological conditions.[11]

Shape-changing fabrics present a new technology that could provide a dynamic alternative to traditional compression modalities. Shape memory alloy (SMA) knitted actuators, SMA filaments deformed into a weft knit fabric structure, are shape-changing fabrics that exhibit surface-wide contraction with an increase in temperature.[1] When integrated into a countermeasure garment, SMA knitted actuators enable a garment to transition between a loose/relaxed (inactive garment state) and tight/stiff (actuated garment state) configuration, on demand. SMA, the active material element, has the ability to recover a remembered shape after deformation with a change in a particular stimulus. Nickel titanium (NiTi) alloys are a type of SMA that exhibit high recovery strains (6–8%) and high recovery stresses (500–900 MPa) in response to changes in temperature, making them excellent thermomechanical actuators.[5] When configured into knit patterns, or consecutive rows and columns of knitted loops, SMA knitted actuators produce complex actuation, such as curling, twisting, and contracting.[1] Two weft knit patterns exhibit actuation contraction: 1) the garter knit pattern; and 2) the jersey knit pattern, sometimes called stockinette.[1] Previous work has identified key geometric design parameters that inform kinematic performance of contractile SMA knitted actuator fabrics, those being: 1) wire diameter, and 2) knit index (**Fig. 1A**).[2] The knit index (i_k), similar to the spring index, is a nondimensional parameter defined as the ratio between the enclosed loop area (A) and the wire diameter squared (d^2).[2] While the knit index has been found to linearly correlate with actuation contraction, prior work has not investigated the force capabilities of these multifunctional fabrics when worn around the human body.

This work experimentally maps the force-displacement characteristics of SMA knitted actuators to their performance/compression capabilities in relation to anthropometric data representative of the target population. Through empirical blocked force testing, generated forces (ΔF), defined as the force differential between inactive forces (F_I) and the actuated forces (F_A), are experimentally investigated.

$$\Delta F = F_A - F_I \quad \text{(Eq. 1)}$$

Functional capabilities of a given SMA knitted actuator geometry are then calculated in relation to the body circumference (C), around which it is wrapped.[9] Findings suggest: 1) forces are suitable to reach medically therapeutic compression (i.e., 18 mmHg),[9] and 2) forces are large enough to satisfy the medical requirements for an orthostatic intolerance garment (i.e., 40–80 mmHg).[8]

METHODS

Prototype Fabrication

To evaluate a range of SMA knitted actuator forces, 10 samples were fabricated using varying geometric design parameters (diameters, d = 0.127 mm, 0.203 mm, 0.381 mm; knit indices, i_k = 39 mm^2/mm^2, 64 mm^2/mm^2, 124 mm^2/mm^2, 138 mm^2/mm^2).[2] Each geometric design combination was knit in both garter and jersey knit patterns in 15 course by 15 wale dimensions (see Fig. 1A) on either a Taitexma TH-860 or TH-260 (Taipei, Taiwan). For prototyping purposes, 90°C Flexinol® wire (Dynalloy, Inc., Irvine, CA, USA) was used as the functional material filament. Above 76°C (material austenite state), 90°C Flexinol® is fully actuated and fully inactive below 23°C (material martensite state).[2] While these transition temperatures are not appropriate for on-body use, prior work has found that custom NiTi-based SMA chemistries with lower transformation temperatures (e.g., NiTi#4, Fort Wayne Metals, Fort Wayne, IN, USA; actuated above 41°C) exhibit comparable behavior to Flexinol® when configured into SMA knitted actuator fabrics despite differences in thermal transition temperatures.[3] Consequently, future applications and systems design work can substitute different NiTi-based SMA materials into a knitted system and achieve comparable blocked force behavior. Each sample underwent a thermomechanical architectural shakedown, a structural settling process that enables repeatable macroscopic actuation performance.[2]

Procedure

Actuator forces were observed through displacement-controlled testing, sometimes referred to as active blocking-force thermal testing. The displacement control test was designed to experimentally investigate changes in sample tension under predetermined displacement when thermally loaded and unloaded. The testing procedure is useful for the application because it provides a controlled method to simulate a condition in which SMA knitted actuators are wrapped around the body at different levels of initial tightness (pretension) and actuated by a change in temperature (see **Fig. 1B**). The method was accomplished by locking an actuator sample at a fixed stretched length and exposing the sample to dynamic thermal loading and unloading. The displacement-controlled test enables observation of inactive forces ($F_{I,n}$) and actuated forces ($F_{A,n}$) for any stretched fabric length (L_n) for each repeated thermal cycle (**Fig. 1C**).

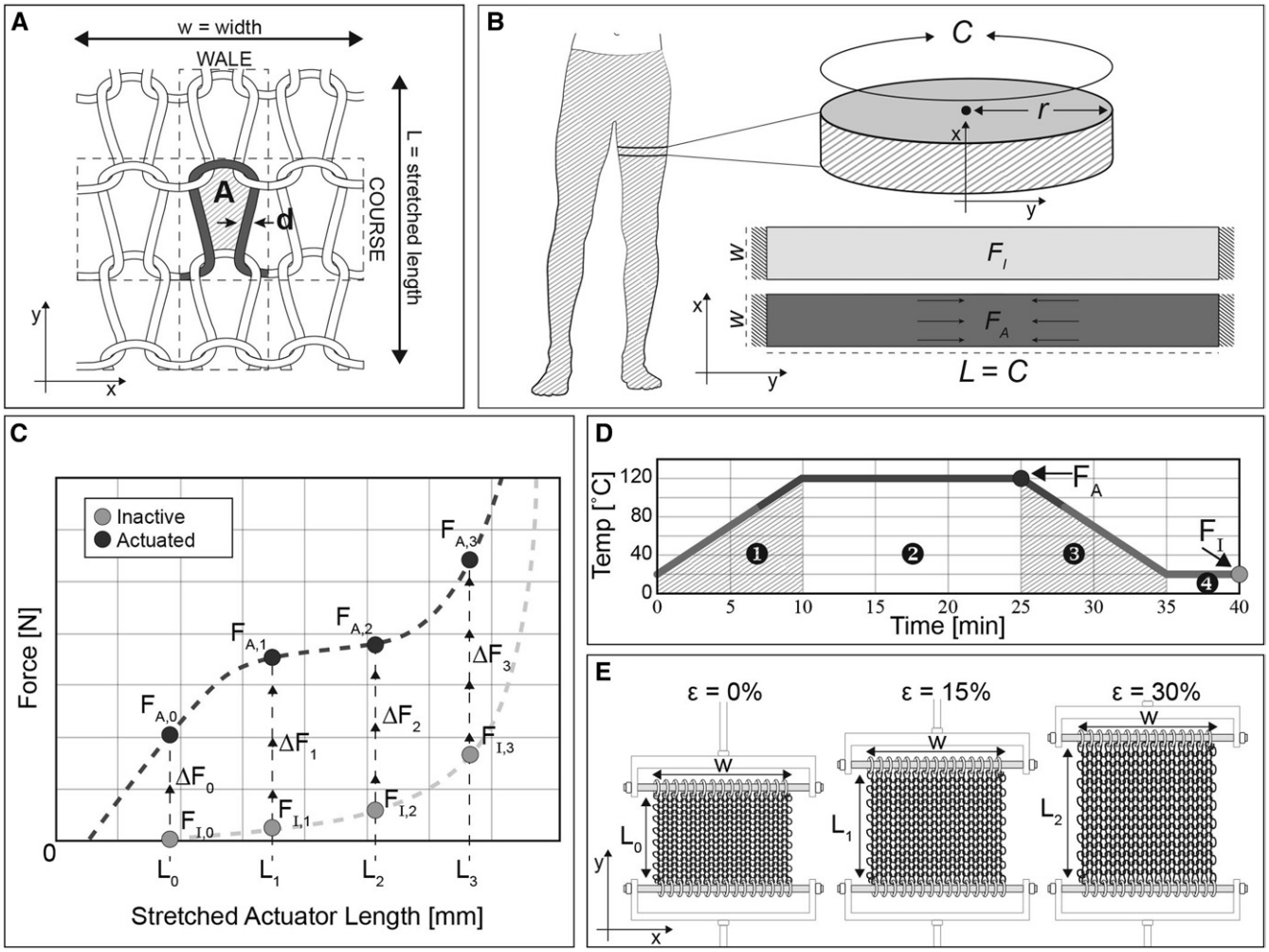

Fig. 1. A) Shape memory alloy (SMA) actuator performance is dependent on two geometric design parameters: wire diameter (d) and knit index (i_k), the ratio of the loop enclosed area (A) to the squared wire diameter (d^2).[2] B) SMA knitted actuators are wrapped around the body such that the actuator x-axis runs along the length of the body to produce circumferential contraction. C) A displacement-control test characterizes the difference between the SMA knitted actuator's maximum actuated force ($F_{A,n}$) and corresponding inactive force ($F_{I,n}$), or the generated force ($\Delta F_n = F_{A,n} - F_{I,n}$), for each stretched actuator length (L_n). D) Repeated thermal cycling is designed to observe the actuator's actuated force (F_A) and inactive force (F_I), repeatedly. E) Each actuator is exposed to thermal cycling at multiple stretched lengths (L_n), or structural strain values, in relation to the inactive origin length ($L_{I,0}$).

Displacement control testing was conducted using a custom load frame housed inside a thermal chamber (Cincinnati Sub Zero, Weiss Technik North America, Inc., Cincinnati, OH, USA) equipped with a linear encoder (200 CPI, U.S. Digital, Vancouver, WA, USA), a temperature-compensated 5-lb load cell (M34 Honeywell, Charlotte, NC, USA; accuracy 0.15%/0.20% full scale) and multiple thermocouples. To begin at an inactive origin length ($L_{I,0}$) under no load, the knit sample was placed in the thermal chamber below the inactive temperature ($T_I = 20°C$), and the sample was displaced until the load cell registered a low force ($F \approx 0.02$ N). The distance between the two grips was then mechanically locked to prevent further displacement. Controlled thermal cycling was repeated three times for each blocked length. Each thermal cycle followed an identical profile (**Fig. 1D**). 1) The temperature was increased at a rate of $10°C \cdot min^{-1}$ to a temperature above the actuated temperature ($T_A = 120°C$). 2) The sample soaked above the actuated temperature for 15 min, after which the actuated force (F_A) was recorded. 3) The chamber was cooled to 20°C at a rate of $10°C \cdot min^{-1}$ and 4) remained cool for an additional 5 min, after which the inactive force (F_I) was recorded. In addition to the inactive origin length ($L_{I,0}$ = 0% strain reference), each sample was characterized at 15%, 30%, and 45% structural strain, represented by stretched knit lengths L_1, L_2, and L_3 (**Fig. 1E**).

Analysis

Post-test analyses were designed to translate experimentally obtained SMA knitted actuator data into on-body compression approximations guided by medical compression hosiery quality and test specifications.[9] Specifically, once the force-strain relationship of SMA knitted actuators are characterized, it is possible to approximate how a compression garment might behave on an individual, pre- and post-actuation, by calculating the magnitude of pressure that can be generated around any cross-sectional circumference. Actuated forces from each of the three thermal cycles ($F_{A,n,cycle1}$, $F_{A,n,cycle2}$, $F_{A,n,cycle3}$) for each stretched

length (L_n) were averaged across cyclic actuation trials to produce an average actuated force per stretched length ($F_{A,n}$).

When normalized by the sample x-axis width (w), each actuated force (F_A,) can be expressed as actuated tension per unit width (t_A) for any stretched length (L_n).

$$t_{A,n}\left[\frac{N}{m}\right]=\frac{F_{A,n}[N]}{w[m]}=\frac{\left(F_{A,n,cycle1}[N]+F_{A,n,cycle2}[N]+F_{A,n,cycle3}[N]\right)}{3w[m]} \quad \text{(Eq. 2)}$$

The maximum actuation force observed across stretched lengths $\left(\hat{F}_A\right)$ and calculated maximum actuated unit tension $\left(\hat{t}_A\right)$ was used as the basis of the analysis. Furthermore, the actuated pressure (p_A) potential of each contractile SMA knitted actuator can be defined by the relationship between the fabric's maximum actuated unit tension $\left(\hat{t}_A\right)$ and any given cross-sectional circumference (C).

$$p_A[Pa]=\frac{\hat{t}_A[N/m]}{C[m]/2\pi};\ P_A[mmHg]=P_A\frac{[Pa]*0.0075[mmHg]}{1[Pa]} \quad \text{(Eq. 3)}$$

Based on the hoop stress equation, Eq. 3 expresses pressure through the relationship between limb circumference and unit tension.[9]

RESULTS

The results demonstrate that stretched SMA knitted actuators produce large actuation forces (F_A) upon an increase in temperature. **Fig. 2A** depicts the temperature-force relationship of two SMA knitted actuators (i.e., #3G and #3J) to demonstrate the raw data obtained from each sample. Three repeatable, counterclockwise thermomechanical passages are indicated by arrows and the actuated and inactive force ($F_{A,n}$; $F_{I,n}$) for each stretched knit length (L_n) are indicated by circular markers. At higher strains, the initial heating passage took a higher force path before falling into repeatable cycles and was not used in the inactive force calculation. Inactive and actuated forces for each stretched length are represented in adjacent plots in relation to stretched actuator length (Fig. 2A).

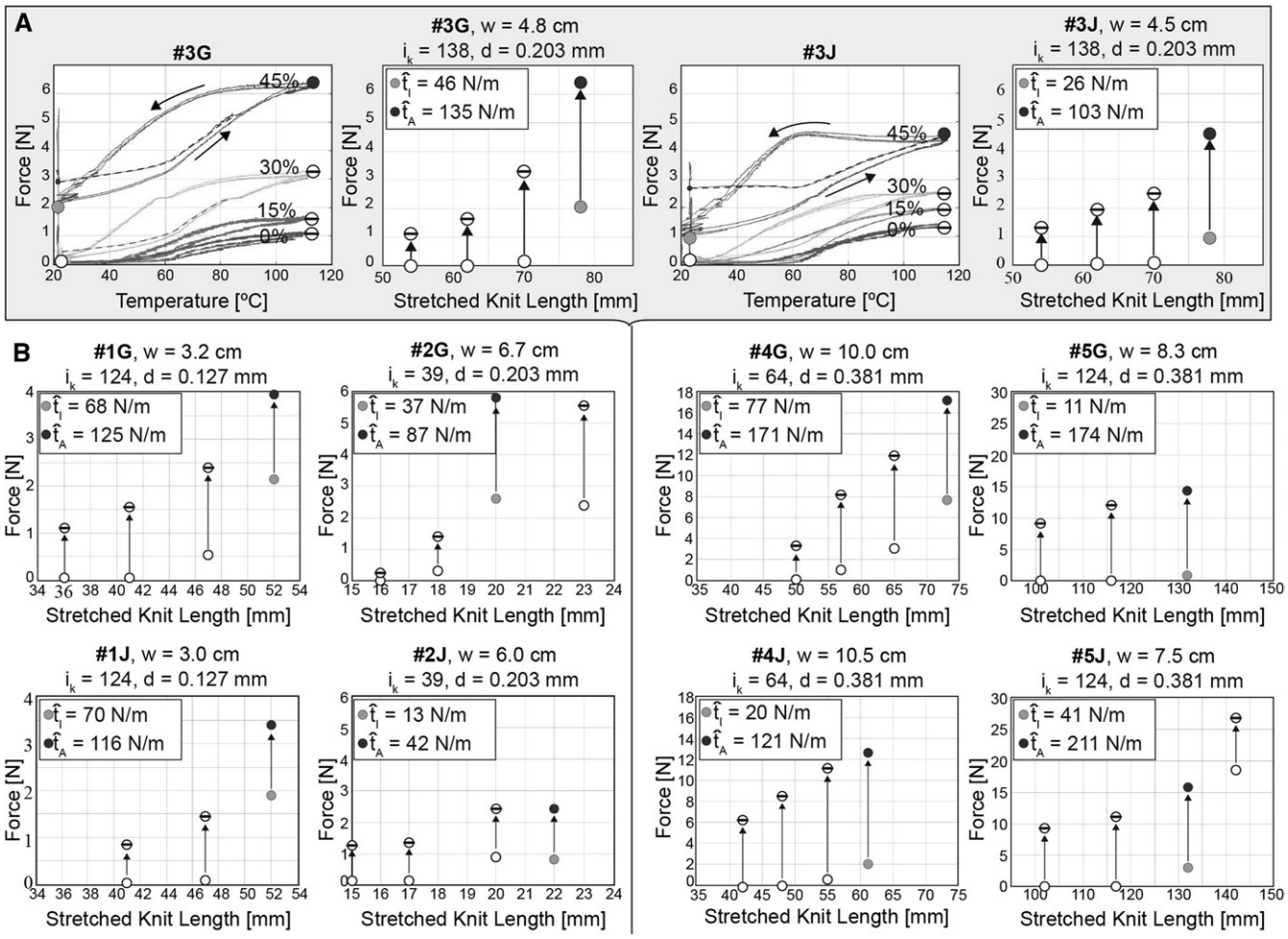

Fig. 2. A) Displacement-control testing results depict a force increase in response to a temperature increase, a trend that magnifies with increasing structural strain. Inactive forces ($F_{I,n}$) and actuated forces ($F_{A,n}$) per stretched knit length (L_n) are depicted for samples #3G and #3J. Maximum actuated unit tension $\left(\hat{t}_A\right)$ is determined by normalizing the maximum actuated force across stretched lengths $\left(\hat{F}_A\right)$ by the sample width (w). B) Actuated forces ($F_{A,n}$) and inactive forces ($F_{I,n}$) for remaining samples for each stretched knit length (L_n). The maximum actuated unit tension $\left(\hat{t}_A\right)$ and corresponding inactive tension $\left(\hat{t}_I\right)$ for each sample are calculated from experimental force data.

Results of the displacement control tests show that increasing structural strain to L_3 usually enables SMA knitted actuators to reach a maximum actuated force $\left(\hat{F}_A\right)$, as well as a maximum generated force $\left(\hat{F}_A - \hat{F}_I = \Delta\hat{F}\right)$, although some samples reached their maximum generated force at L_2 (i.e., #2G, #5J) and other samples could not be strained to L_3 (i.e., #5G, #1J). Sample #4J was tested at 39% strain, the maximum strain possible. The maximum actuated forces $\left(\hat{F}_A\right)$ ranged from 2.5–17.1 N across samples (SE 0.01–0.40 N) and the average inactive forces that corresponded with maximum average actuated forces $\left(\hat{F}_I\right)$ ranged from 0.8–7.7 N, excluding L_3 for samples #2G and #5J, which exhibited reduced generated force in relation to L_2. The maximum generated force $\left(\Delta\hat{F}\right)$ ranged from 1.4–13.5 N (SE 0.01–0.20 N). Higher actuated forces (F_A) were observed with larger wire diameter actuators (**Fig. 2B**, #4G, #4J, #5G, #5J).

Inactive unit tension (t_I) and actuated unit tension (t_A) for each stretched length (L_n) were calculated according to Eq. 2. Fig. 2 depicts each sample's maximum actuated unit tension $\left(\hat{t}_A\right)$, usually observed at L_3, and the corresponding inactive unit tension $\left(\hat{t}_I\right)$. Maximum actuated unit tensions $\left(\hat{t}_A\right)$ were 42-211 $\mathrm{N \cdot m^{-1}}$ while corresponding inactive unit tensions $\left(\hat{t}_I\right)$ were 11-77 $\mathrm{N \cdot m^{-1}}$ across all samples. The maximum generated unit tensions $\left(\Delta\hat{t} = \hat{t}_A - \hat{t}_I\right)$ ranged from 29-170 $\mathrm{N \cdot m^{-1}}$, with an average of 88 $\mathrm{N \cdot m^{-1}}$.

Fig. 3A depicts pressure values calculated according to Eq. 3 in relation to changing circumferences (e.g., 0–115 cm). To evaluate functional capabilities for a countermeasure garment, data from the Anthropometric Survey of U. S. Army Personnel (ANSUR 2012), which is representative of women and men who rely on aerospace compression garments, was used to approximate body cross-sectional circumferences (C)

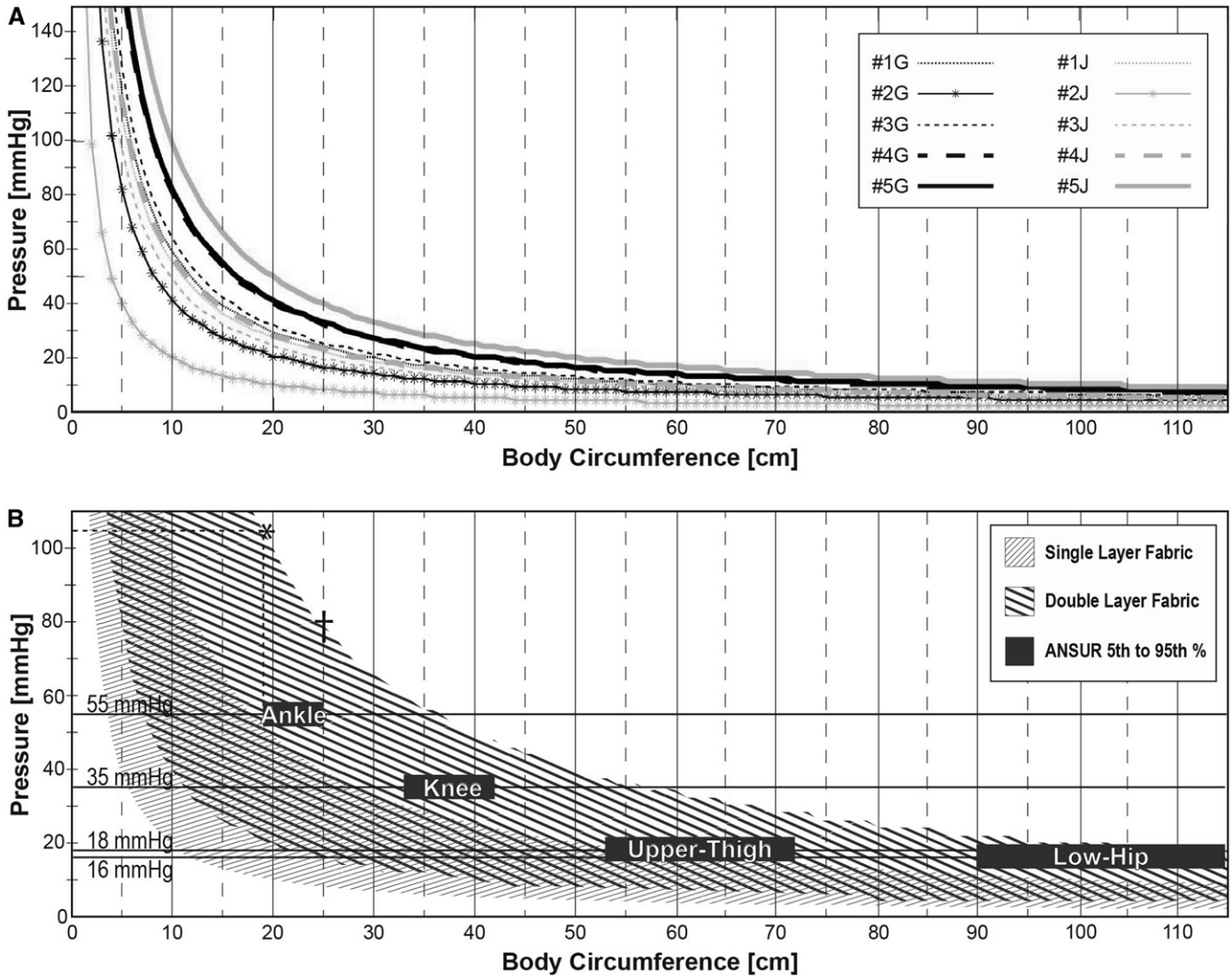

Fig. 3. A) Maximum actuated unit tension $\left(\hat{t}_A\right)$ for each sample evaluated in relation to body circumference (C) to observe actuated pressure potential (p_A). B) Theoretical pressure potential of SMA knitted actuators (single and double-layered) evaluated in relation to anthropometric data for an aerospace population (*5th-% women to †95th-% men, ANSUR 2012). Pressure specifications per body location (i.e., 55 mmHg ankle, 35 mmHg knee, 18 mmHg thigh, 16 mmHg abdomen) are used for comparative purposes only and were informed by prior clinical testing conducted in NASA Johnson Space Center's Cardiovascular Lab.[11]

for the population (**Fig. 3B**). Actuated pressure (p_A), inactive pressure (p_I), and generated pressure ($\Delta p = p_A - p_I$), defined by the difference between inactive compression (p_I) and actuated compression (p_A), were calculated to approximate dynamic compression behaviors, specifically increases in on-body pressure, according to Eq. 3. **Table I** provides a full report of inactive and actuated compression ranges for SMA knitted actuators and shows that low, inactive compression values would be applied to the body before garment actuation ($p_I < 20$ mmHg in all areas of the lower body except the ankle).

The range of compression capabilities summarized in Table I are calculated using upper and lower bounds, specifically: 1) the largest actuated unit tension value of all tested SMA knitted actuator samples $\left(\hat{t}_{A,\#5J} = 211\ \mathrm{N \cdot m^{-1}}\right)$ when wrapped around the smallest ankle circumference (5th% women, ANSUR); and 2) the smallest actuated unit tension value $\left(\hat{t}_{A,\#2J} = 42\ \mathrm{N \cdot m^{-1}}\right)$ when wrapped around the largest ankle circumference (95th% men, ANSUR). Double layered calculations are included that ignore system friction and double the maximum austenite actuated unit tension values $\left(2*\hat{t}_{A,\#5J} = 422\ \mathrm{N \cdot m^{-1}}; 2*\hat{t}_{A,\#2J} = 84\ \mathrm{N \cdot m^{-1}}\right)$ to evaluate the compression capability of double-layered actuator fabrics because previous work has shown that SMA knitted actuators approximately double in force in a layered configuration.[2]

Theoretical performance capabilities of an actuated system (p_A) ranged from 8–52 mmHg at the ankle (single layer fabric) to 16–105 mmHg at the ankle (double layer fabric) (Fig. 3B). Compression of an inactive single layer system (p_I) ranged from 2–19 mmHg at the ankle to 4–38 mmHg in a double layer configuration. Dynamic compression (Δp) ranged from 6–33 mmHg (single layer system) to 12–67 mmHg (double layer system) at the ankle. Consequently, to reach a maximum actuated compression value of 52 mmHg around the smallest ankle circumference (5th% women, ANSUR), the body would initially experience inactive (passive) compression of 19 mmHg. Upon actuation, the garment tension would increase, causing a pressure increase of 33 mmHg.

DISCUSSION

The analysis shows that SMA knitted actuators generate enough force to satisfy the NASA Commercial Crew Transportation Requirements Document CCT-REQ-1130, with calculated pressures reaching up to 105 mmHg (5th% women, ANSUR) to 79 mmHg (95th% men, ANSUR), as shown in Fig. 3B. In addition to astronaut countermeasure garments, the study reveals that SMA knitted actuators have therapeutic potential for high-performance aircraft applications and a spectrum of terrestrial medical disorders such as postural orthostatic tachycardia syndrome (30–40 mmHg), orthostatic hypotension (25–30 mmHg), lymphedema (15–50 mmHg), and deep vein thrombosis (40–50 mmHg). With advancements in force capabilities, SMA knitted actuators could also be considered in the design of mechanical counterpressure spacesuits (222 mmHg), a theoretical alternative to gas-pressurized extravehicular activity suits.[4]

Operationally, these actuators enable future compression garments to begin looser around the body ($p < 20$ mmHg) and become tighter ($p > 20$ mmHg) with an increase in temperature. In addition to fine-tuning compression levels, dynamic fabrics also allow a garment to compensate for spaceflight-induced dimensional change caused by fluid shifts, muscle atrophy, and even lean muscle mass increase. The magnitude of pressure increase is informed by user anthropometry in relation to: 1) SMA knitted actuator geometry, 2) inactive pretensioning around the body, and 3) the magnitude of temperature increase. Within a garment system, compression can be modified in three ways: 1) swapping out modular actuator panels (e.g., low-, medium-, high-force) that can zip on/off a base garment; 2) adjusting actuator pretension through garment lacing or modular zipper inserts; or 3) regulating the magnitude of thermal input. As shown in prior work, displacement-control testing demonstrated that pretensioning (i.e., increasing structural strain) around the body cross-section is required for the SMA knitted actuator system to reach maximum actuated forces and reach full generated force potential.[4] In other words, the penalty for higher maximum actuated compression is a higher starting inactive pressure. Future work will investigate structural modifications to SMA knitted actuators to decrease starting, passive forces and increase maximum actuated forces.

Table I. Calculated Actuated Pressure Potential (p_A) and Inactive Pressure Potential (p_I) of SMA Knitted Actuators in Relation to Low-Body Circumferences Gathered from the 2012 Anthropometric Survey of U. S. Army Personnel, Specifically 5th Percentile Female to 95th Percentile Male Dimensions.

		SINGLE LAYER		DOUBLE LAYER		
BODY CROSS-SECTION (C)	ANSUR 5TH–95TH% RANGE (cm)*	P_I (mmHg)	P_A (mmHg)	P_I (mmHg)	P_A (mmHg)	NASA CARDIO LAB PRESSURE[11] (mmHg)
Ankle	19–25	2–19	8–52	4–38	16–105	55
Knee†	33–42	1–11	5–30	2–22	9–60	35
Low-Thigh	35–47	1–10	4–28	2–21	8–57	18
Upper-Thigh	53–72	1–7	3–19	1–14	5–38	18
Low-Hip	90–116	0–4	2–11	1–8	3–22	16
Waist	71–113	0–5	2–14	1–10	4–28	16

* Combines women and men.

† Knee measurements were taken from the NASA Anthropometric Sourcebook.

In an OI garment (and other systems), the operational system concept is reliant on SMA material transformation temperatures. Prior work details a custom SMA material that would enable a reduced-power countermeasure garment to mitigate thermal discomfort and system power requirements.[3] In this instance, 1) the garment would be donned in a relaxed configuration in ambient cabin temperatures ($T_{cabin} = 20°C$) under the Orion Crew Survival Suit before prelanding activities begin. 2) Upon warming to skin temperature ($T_{skin} \approx 30°C$), the garment would remain inactive, applying passive pressure less than 20 mmHg. This low-pressure state would remain stable while the crewmember is seated in the capsule, improving crew comfort during the several-hour waiting period before landing activities are initiated. 3) Once landing activities begin, the crewmembers activate their countermeasure garment through resistive heating up to 40°C, NASA's maximum allowable touch temperature, using a battery pack housed outside the Orion Crew Survival Suit.[10] System pressure increase could be attained by controlling thermal input—heating first to 35°C, followed by 40°C if more compression is required. Once warmed, the heat/power is removed and the garment remains fully actuated upon equilibration with the skin's temperature ($T_{skin} \approx 30°C$). 4) The garment would be worn fully actuated through landing activities and for several days postlanding without additional heat/power. 5) The garment would be doffed with the aid of zipper releases and placed in a freezer to return the garment to an inactive state before reuse. While the operational concept minimizes system power requirements, the tradeoff is the inability to reduce or turn off compression—it can only be increased and/or maintained. Future work will investigate methods on the material, actuator, and systems level to enable the user to reduce compression level during use.

As SMA knitted actuator prototypes are realized and operational concepts are evaluated, future work will require on-body pressure testing to demonstrate dynamic compression capabilities in a worn system. Projections of compression capabilities around circumferential body cross-sections are presently theoretical and only suggest functional potential in the proposed application. While the methods by which medical compression classes are calculated (i.e., Eq. 3) are regulatory standard for ready-to-wear and custom medical compression garments and make predictions easier, these methods are less accurate than on-body pressure testing due to assumptions, such as perfect cylinders, rigid and static bodies, and frictionless conditions.[9] Future work will integrate SMA knitted actuators into compression garment prototypes to realize a low-profile, dynamic approach to traditional aerospace compression modalities that mitigates the mobility concerns of pneumatic garments and addresses the don/doff challenges of elastic garments. This research enables a new generation of smart material-based dynamic compression technologies that can achieve fully integrated (i.e., no need for joining cartridges or snaps) spatial actuation around the human body.

ACKNOWLEDGMENTS

A special thank you goes to members of NASA's Johnson Space Center as well as University of Minnesota peers from the Wearable Technology Lab (WTL) and the Design of Active Materials and Structures Lab (DAMSL).

Trade names and trademarks are used in this report for identification only. Their usage does not constitute an official endorsement, either expressed or implied, by the National Aeronautics and Space Administration.

Financial Disclosure Statement: This work was supported by a NASA OTC Space Technology Research Fellowship (grant number 80NSSC17K0158) as well as by MnDRIVE RSAM. The authors have no competing interests to declare.

Authors and affiliations: Rachael Granberry, M.S., Kevin Eschen, M.S., Julianna Abel, Ph.D., and Brad Holschuh, Ph.D., University of Minnesota, Minneapolis, MN, USA, and Amy Ross, M.S., NASA Johnson Space Center, Houston, TX.

REFERENCES

1. Abel J, Luntz J, Brei D. Hierarchical architecture of active knits. Smart Mater Struct. 2013; 22(12):125001.
2. Eschen K, Granberry R, Abel J. Guidelines on the design, characterization, and operation of shape memory alloy knitted actuators. Smart Mater Struct. 2020; 29(3):035036.
3. Granberry R, Padula II S, Eschen K, Abel J, Holschuh B. Design and control of reduced power actuation for active-contracting orthostatic intolerance garments. Proceedings of the 49th International Conference on Environmental Systems; 2019 July 8-11, Boston, MA. Lubbock (TX, USA): Texas Tech University; 2019.
4. Holschuh BT, Newman DJ. Morphing compression garments for space medicine and extravehicular activity using active materials. Aerosp Med Hum Perform. 2016; 87(2):84–92.
5. Lagoudas DC. Shape memory alloys: modeling and engineering applications. New York: Springer Science+Business Media, LLC; 2008.
6. Lee SMC, Feiveson AH, Stein S, Stenger MB, Platts SH. Orthostatic intolerance after ISS and space shuttle missions. Aerosp Med Hum Perform. 2015; 86(12, Suppl.):A54–A67.
7. Lee SM, Guined JR, Brown AK, Stenger MB, Platts SH. Metabolic consequences of garments worn to protect against post-spaceflight orthostatic intolerance. Aviat Space Environ Med. 2011; 82(6):648–653.
8. Leuders KL. ISS crew transportation and services requirements document CCT-REQ-1130. Merritt Island (FL, USA): John F. Kennedy Space Center, Commercial Crew Program; 2015.
9. Medical Compression Hosiery. Quality Assurance RAL-GZ 387/1. Bonn (Germany): RAL German Institute for Quality Assurance; 2008.
10. National Aeronautics and Space Administration. NASA space flight human system standards. NASA-STD-3001. Washington (DC): NASA; 2017.
11. Stenger MB, Lee SMC, Westby CM, Ribeiro LC, Phillips TR, et al. Abdomen-high elastic gradient compression garments during post-spaceflight stand tests. Aviat Space Environ Med. 2013; 84(5):459–466.
12. Waters WW, Ziegler MG, Meck JV. Postspaceflight orthostatic hypotension occurs mostly in women and is predicted by low vascular resistance. J Appl Physiol. 2002; 92(2):586–594.